

Accurate and Efficient World Modeling with Masked Latent Transformers

Maxime Burchi¹ Radu Timofte¹

Abstract

The Dreamer algorithm has recently obtained remarkable performance across diverse environment domains by training powerful agents with simulated trajectories. However, the compressed nature of its world model’s latent space can result in the loss of crucial information, negatively affecting the agent’s performance. Recent approaches, such as Δ -IRIS and DIAMOND, address this limitation by training more accurate world models. However, these methods require training agents directly from pixels, which reduces training efficiency and prevents the agent from benefiting from the inner representations learned by the world model. In this work, we propose an alternative approach to world modeling that is both accurate and efficient. We introduce EMERALD (Efficient MaskEd latent tRAnsformer worLD model), a world model using a spatial latent state with MaskGIT predictions to generate accurate trajectories in latent space and improve the agent performance. On the Crafter benchmark, EMERALD achieves new state-of-the-art performance, becoming the first method to surpass human experts performance within 10M environment steps. Our method also succeeds to unlock all 22 Crafter achievements at least once during evaluation. We release our code at <https://github.com/burchim/EMERALD>.

1. Introduction

Model-based reinforcement learning has attracted increasing research attention in recent years (Hafner et al., 2019; 2020; 2021; 2023; Schrittwieser et al., 2020). The growing computational capabilities of hardware systems have allowed researchers to make significant progress, training world models from high-dimensional observations like videos (Yan

¹Computer Vision Lab, CAIDAS & IFI, University of Würzburg, Germany. Correspondence to: Maxime Burchi <maxime.burchi@uni-wuerzburg.de>.

Proceedings of the 42nd International Conference on Machine Learning, Vancouver, Canada. PMLR 267, 2025. Copyright 2025 by the author(s).

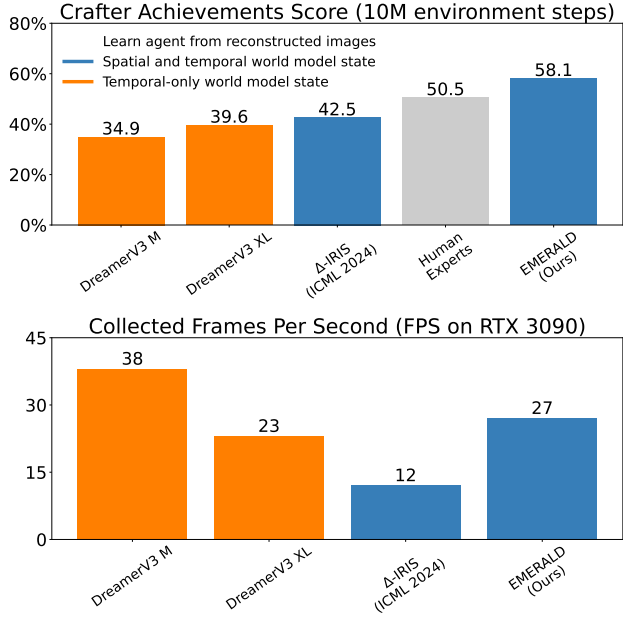


Figure 1: Achievements score and collected Frames Per Second (FPS) of recently published model-based methods on the Crafter benchmark. EMERALD is the first method to exceed the performance of human experts on the benchmark. The world model uses a spatial latent state with MaskGIT predictions to improve performance and training efficiency. Δ -IRIS proposed an accurate world model but suffers from lower training efficiency due to autoregressive decoding in latent space and agent learning from reconstructed images.

et al., 2023) using deep neural networks (LeCun et al., 2015) as function approximations. World models (Sutton, 1991; Ha & Schmidhuber, 2018) summarize the experience of an agent into a predictive function that can be used instead of the real environment to learn complex behaviors. Having access to a model of the environment enables the agent to simulate multiple plausible trajectories in parallel, improving generalization, sample efficiency, and decision-making via planning.

Among these approaches, the Dreamer algorithm (Hafner et al., 2020; 2021; 2023) has achieved remarkable performance in various environments by training a world model to generate imaginary trajectories in latent space. However,

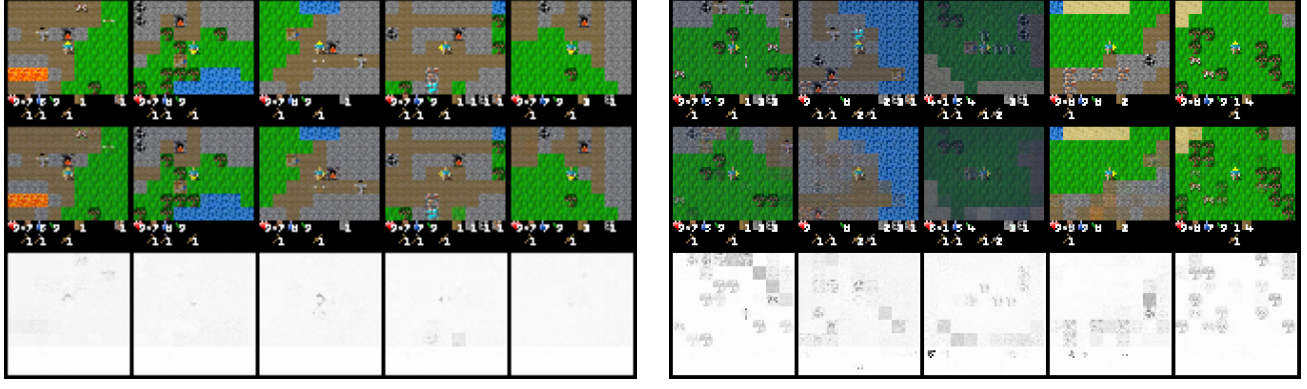


Figure 2: Comparison of EMERALD image reconstruction with DreamerV3. We show the 5 frames with highest reconstruction error among a batch of 1024 test observations. The top row indicates original images, the middle row shows reconstructed images and the bottom row shows reconstruction error. We observe that EMERALD achieves near-perfect reconstruction, with errors resulting mostly from player orientation and textures. DreamerV3 fails to perceive crucial details like diamonds and skeleton arrows, which diminishes the agent’s perception capacity and negatively impacts its performance.

while the world model has no difficulty in simulating simple visual environments such as DeepMind Control (Tassa et al., 2018) tasks or Atari games (Bellemare et al., 2013), some inaccuracies appear when modeling more complex environments like Crafter (Hafner, 2022) and MineRL (Guss et al., 2019). As shown in Figure 2b, the world model has difficulty perceiving important details on Crafter. This failure to learn accurate representations for the agent leads to a lower performance.

To remedy this problem, recent approaches have proposed more accurate world models. Δ -IRIS (Micheli et al., 2024) proposed to encode stochastic deltas for changes in the observation. Concurrently, DIAMOND (Alonso et al., 2024) proposed a diffusion-based world model using a U-Net architecture. Both of these approaches proposed new world model alternatives to improve the reconstruction quality of generated trajectories and increase the agent performance. However, they also require learning the agent from reconstruction images, which impact learning efficiency and does not allow the agent to benefit from inner representations learned by the world model such as long-term memory. This significantly limits the potential of such methods for perception and training efficiency.

In this work, we propose an alternative approach to world modeling that is both accurate and efficient. We introduce EMERALD, a Transformer model-based reinforcement learning algorithm using a spatial latent state with MaskGIT predictions to generate accurate trajectories in latent space and improve the agent performance. Originally designed for vector-quantized image generation (Van Den Oord et al., 2017), MaskGIT (Chang et al., 2022) improves decoding speed and generation quality compared to

autoregressive sequential decoding (Esser et al., 2021). This approach was later adapted by TECO (Yan et al., 2023), demonstrating that MaskGIT-based latent space predictions could enable powerful video generation models. Inspired by these advances, we apply MaskGIT to model-based reinforcement learning, allowing the agent to better perceive crucial environment details while improving decoding efficiency. Furthermore, the agent benefits from internal representations learned by the world model, such as long-term memory, enabling it to track important objects and effectively map the environment. As shown in Figure 1, EMERALD sets a new record on the Crafter benchmark, being the first method to exceed human experts performance within 10M environment steps with a score of 58.1%. Our method also succeeds to unlock all 22 Crafter achievements at least once during evaluation. Additionally, we report results on the commonly used Atari 100k benchmark (Kaiser et al., 2020) to demonstrate the general efficacy of EMERALD on Atari games that do not necessarily require the use of spatial latents to achieve near perfect reconstruction.

2. Related Works

2.1. Model-based Reinforcement Learning

Model-based reinforcement learning approaches use a model of the environment to simulate agent trajectories, improving generalization, sample efficiency, and decision-making via planning. Following the success of deep neural networks for learning function approximations, researchers proposed to learn world models using gradient backpropagation, allowing the development of powerful agents with limited data. One of the earliest model-based algorithms applied to image data is SimPLe (Kaiser et al., 2020), which

Table 1: Comparison between EMERALD and other recent model-based approaches. *Latent* (z_t) refers to image latent representations carrying spatial information while *hidden* (h_t) refers to world model hidden state carrying temporal information. EMERALD uses a spatial latent state to improve world model accuracy. It also trains the agent in latent space to increase efficiency and benefit from world model inner representations. Efficient decoding is performed using MaskGIT.

Attributes	IRIS	DreamerV3	Δ -IRIS	DIAMOND	EMERALD (Ours)
World Model	Transformer	GRU	Transformer	U-Net	Transformer
Tokens	Latent (4×4)	Latent	Latent (2×2)	N/A	Latent (4×4)
Latent Representation	VQ-VAE	Categorical-VAE	VQ-VAE	N/A	Categorical-VAE
Decoding	Sequential	N/A	Sequential	EDM	MaskGIT
Agent State (s_t)	Image	Latent, hidden	Image	Image	Latent (4×4), hidden

proposed a world model for Atari games in pixel space using a convolutional autoencoder architecture. The world model predicts future frames and environment rewards based on past observations and selected actions, enabling the training of a Proximal Policy Optimization (PPO) agent (Schulman et al., 2017) with simulated trajectories.

Concurrently, PlaNet (Hafner et al., 2019) introduced a Recurrent State-Space Model (RSSM) incorporating Gated Recurrent Units (GRUs) (Cho et al., 2014) to learn a world model in latent space, planning using model predictive control. PlaNet learns a convolutional variational autoencoder (VAE) (Kingma & Welling, 2014) with a pixel reconstruction loss to encode observations into stochastic state representations. The RSSM then predicts future stochastic states and environment rewards based on previous stochastic and deterministic recurrent states. Following the success of PlaNet on DeepMind Visual Control tasks, Dreamer (Hafner et al., 2020) improved the algorithm by learning an actor and a value network from the world model hidden representations. DreamerV2 (Hafner et al., 2021) extended the algorithm to Atari games, replacing Gaussian latents by categorical latent states using straight-through gradients (Bengio et al., 2013) to improve performance. Lastly, DreamerV3 (Hafner et al., 2023) mastered diverse domains using the same hyper-parameters with a set of architectural changes to stabilize learning across tasks. The agent uses symlog predictions for the reward and value function to address the scale variance across domains. The networks also employ layer normalization (Ba et al., 2016) to improve robustness and performance while scaling to larger model sizes. It stabilizes policy learning by normalizing the returns and value function using an Exponential Moving Average (EMA) of the returns percentiles. With these modifications, DreamerV3 outperformed specialized model-free and model-based algorithms in a wide range of benchmarks.

Concurrent approaches have proposed to use a Transformer-based world model to improve the hidden representations and memory capabilities compared to RNNs. IRIS (Micheli et al., 2023) first proposed a world model composed of a

VQ-VAE (Van Den Oord et al., 2017) to convert input images into discrete tokens and an autoregressive Transformer to predict future tokens. TransDreamer (Chen et al., 2021) proposed to replace Dreamer’s RSSM with a Transformer State-Space Model (TSSM) using masked self-attention to imagine future trajectories. TWM (Robine et al., 2023) (Transformer-based World Model) proposed a similar approach, encoding states, actions and rewards as distinct successive input tokens for the autoregressive Transformer. More recently, STORM (Zhang et al., 2024) achieved results comparable to DreamerV3 with better training efficiency on the Atari 100k benchmark.

2.2. Accurate World Modeling in Pixel Space

Another line of work focuses on designing accurate world models to train agents from reconstructed trajectories in pixel space. Analogously to SimPLe, the agent’s policy and value functions are trained from image reconstruction instead of world model hidden state representations. This requires learning auxiliary encoder networks for the policy and value functions. Micheli et al. (2024) proposed Δ -IRIS, encoding stochastic deltas between time steps using previous action and image as conditions for the encoder and decoder. This increased VQ-VAE compression ratio and image reconstruction capabilities, achieving state-of-the-art performance on the Crafter (Hafner, 2022) benchmark.

Meanwhile, DIAMOND (Alonso et al., 2024) introduced a diffusion-based (Sohl-Dickstein et al., 2015) world model with EDM decoding (Karras et al., 2022) to generate high-quality trajectories and improve the agent performance. The paper demonstrated that diffusion can successfully be applied to world modeling, requiring as few as 3 denoising steps for imagination. The method was evaluated on the Atari 100k benchmark showing better reconstruction quality and improved performance compared to DreamerV3. However, it was not applied to a memory-demanding benchmark like Crafter that requires both good memory and visual perception to achieve strong results. The authors disclosed that initial experiments on the Crafter benchmark did not

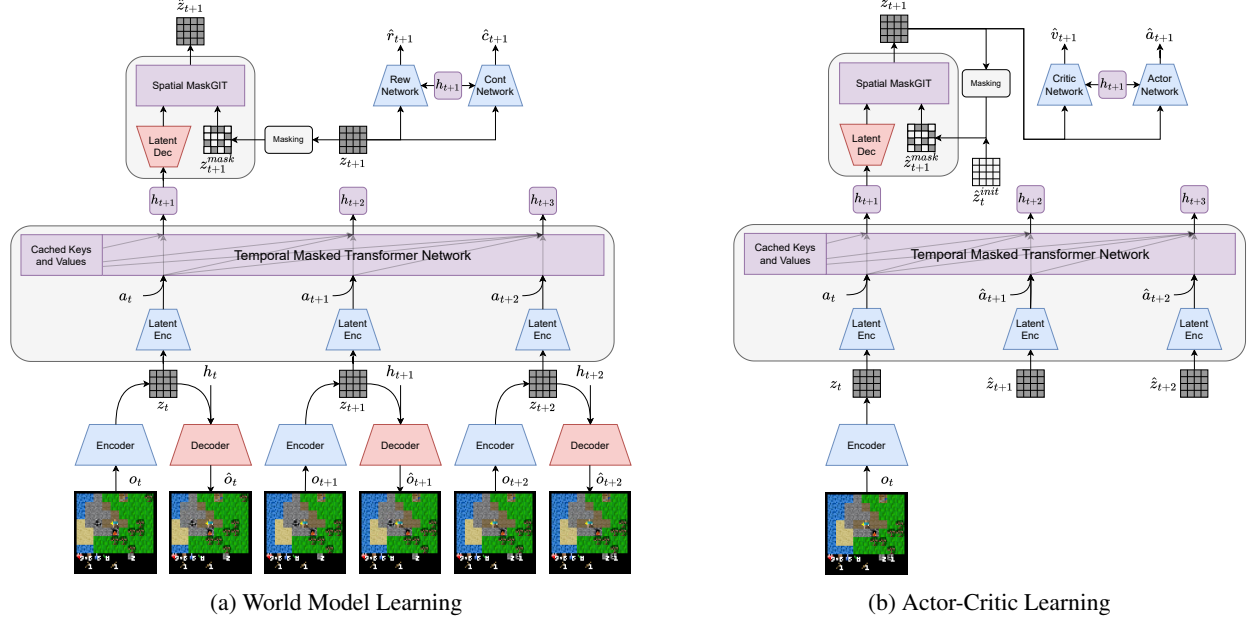


Figure 3: Efficient masked latent Transformer-based world model. EMERALD uses a spatial latent state z_t and a temporal hidden state h_t to model the environment accurately and effectively. The world model predictions are made using a spatial MaskGIT predictor network to increase decoding speed while maintaining accuracy. Actor-critic learning is performed by imagining trajectories in latent space which allows the agents to benefit from world model inner representations.

achieve good performance due to the absence of an effective memory module for the world model. We find that DIAMOND has difficulties predicting future frames in Crafter, generating hallucinations. In this work, we propose to improve performance and training efficiency by learning an accurate world model in latent space. Table 1 compares the architectural details of recent model-based approaches with our proposed method.

2.3. Scheduled MaskGIT Predictions in Latent Space

Parallel tokens prediction with refinements was introduced by MaskGIT (Masked Generative Image Transformer) (Chang et al., 2022) as an alternative to sequential decoding for vector quantized image generation (Van Den Oord et al., 2017; Ramesh et al., 2021; Esser et al., 2021). MaskGIT proposed to replace autoregressive decoding with scheduled parallel decoding of masked tokens to improve generation quality and significantly decrease decoding time. During training, the method samples decoding times $\tau \in [0, 1]$ uniformly. It proceeds to mask $N = \lfloor \gamma HW \rfloor$ tokens where $\gamma = \cos(\frac{\pi}{2}\tau)$ follows a cosine schedule and H and W correspond to the height and width of the latent space in tokens. At decoding time, the model is sampled to progressively predict all the tokens. This is done by selecting the most probable tokens and masking the remaining tokens for the next decoding step.

Inspired by the success of MaskGIT and similar approaches such as draft-and-revise (Lee et al., 2022) for image generation, Yan et al. (2023) proposed TECO (Temporally Consistent Video Transformer). TECO is a video generation model using MaskGIT with draft-and-revise decoding to predict future frames in latent space. They showed that using a MaskGIT prior allows for not just faster but also higher quality sampling compared to an autoregressive sequential prior. Using a pre-trained VQ-GAN (Esser et al., 2021) vector quantizer, the algorithm demonstrated strong memory capabilities and generation quality. In this work, we propose to apply MaskGIT to model-based reinforcement learning. We train a world model that is both accurate and efficient without requiring pre-trained discrete representations.

Meanwhile, the use of MaskGIT as prior for model-based reinforcement learning was concurrently explored by GIT-STORM (Meo et al., 2024). GIT-STORM proposed to apply MaskGIT decoding using a draft-and-revise strategy to the recently proposed STORM model. However, we note that the motivation behind GIT-STORM is different from our work: Similarly to image and video generation works (Chang et al., 2022; Yan et al., 2023), EMERALD uses MaskGIT as an alternative to sequential token decoding in order to improve decoding efficiency for spatial latent spaces. In contrast, the GIT-STORM paper applied MaskGIT to the vector latent space of STORM in order to improve the quality of sampling. Key differences also lie in

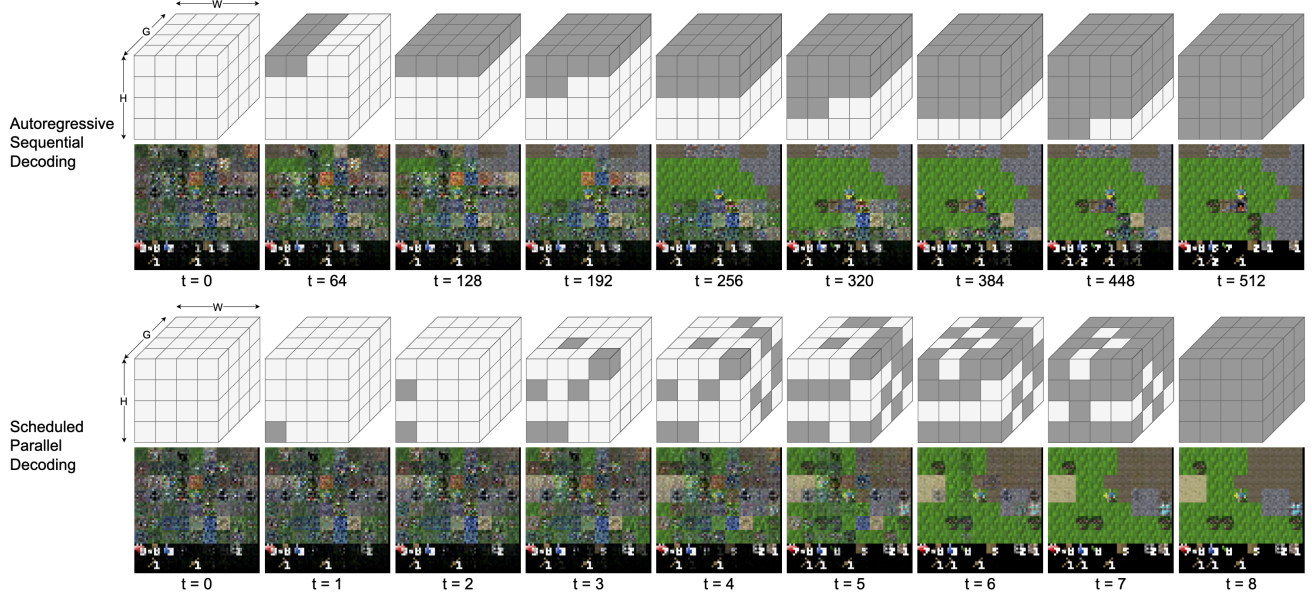


Figure 4: Comparison of scheduled parallel decoding in EMERALD vs. autoregressive sequential decoding used by IRIS and Δ -IRIS. We illustrate the $H \times W \times G$ latent space of our method with only 4 of the 32 groups for better clarity. Sequential decoding predicts one token at a time, significantly impacting efficiency. In contrast, EMERALD uses parallel predictions with scheduled refinements, reducing decoding time while preserving the coherence of predicted tokens.

the architecture of the MaskGIT network. GIT-STORM performs attention on the 32 feature tokens of the vector latent space while EMERALD first concatenates the tokens along the feature dimension and performs attention on spatial positions similarly to the original MaskGIT paper (Chang et al., 2022).

3. Method

We introduce EMERALD, a Transformer model-based reinforcement learning algorithm using a spatial latent state with MaskGIT predictions to generate accurate trajectories in latent space and improve the agent performance. EMERALD can be separated into three main components: The Transformer world model that learns to simulate the environment in latent space. A critic network that learns to estimate the sum of future rewards. And an actor network that learns to select actions that maximize future rewards estimated by the critic network. Each component is trained concurrently by sampling trajectories from a replay buffer of past experiences. This section describes the architecture and optimization process of our proposed masked latent Transformer world model. Additionally, we provide a brief overview of the imagination process for actor-critic learning. Figure 3 provides a visual overview of world model learning and imagination process during the actor-critic learning phase.

3.1. World Model Overview

Analogously to the Dreamer algorithm (Hafner et al., 2023) and other recent approaches learning a world model in latent space (Robine et al., 2023; Zhang et al., 2024), we encode input image observations o_t into hidden representations using a convolutional VAE with categorical latents. To balance prediction accuracy and efficiency, our world model adopts a carefully designed architecture with spatial latent states z_t and temporal hidden states h_t . The spatial latent states are first projected into temporal feature vectors for efficient processing by the world model. A temporal Transformer network with masked self-attention then generates the temporal hidden states h_t by modeling long-range dependencies. These temporal states are subsequently projected back into spatial features for MaskGIT predictions. The trainable components of the world model are the following:

$$\begin{aligned}
 \text{Encoder Network: } & z_t \sim q_\phi(z_t \mid o_t) \\
 \text{Transformer Network: } & h_t = f_\phi(z_{1:t-1}, a_{1:t-1}) \\
 \text{MaskGIT Predictor: } & \hat{z}_t \sim p_\phi(\hat{z}_t \mid h_t, z_t^{mask}) \\
 \text{Decoder Network: } & \hat{o}_t \sim p_\phi(\hat{o}_t \mid h_t, z_t) \\
 \text{Reward Predictor: } & \hat{r}_t \sim p_\phi(\hat{r}_t \mid h_t, z_t) \\
 \text{Continue Predictor: } & \hat{c}_t \sim p_\phi(\hat{c}_t \mid h_t, z_t)
 \end{aligned} \tag{1}$$

The spatial latent states and temporal hidden states are combined to form the world model state $s_t = [z_t, h_t]$, which integrates both spatial and temporal information. Latent state predictions are made using a spatial MaskGIT network,

while separate networks predict the environment reward \hat{r}_t and episode continuation \hat{c}_t .

Encoder Network While previous approaches project encoder features to a compressed vector latent space to simplify world model predictions, our method leverages a spatial latent space to improve world model accuracy and the agent performance. The spatial feature representations are first projected to categorical distribution logits $l \in \mathbb{R}^{H \times W \times D}$, which are then reorganized into multiple feature groups G for sampling. Instead of representing entire latent vector with a single embedding, the token representations combine embeddings from multiple feature groups. This grouping mechanism was originally used by DreamerV2 (Hafner et al., 2021) to improve training stability using a flexible latent representation. We sample discrete stochastic states $z_t \in \mathbb{R}^{H \times W \times G \times (D/G)}$ from the encoder, which serves as spatial latent states for our world model.

The use of a spatial latent space allows to effectively improve the accuracy of the world model without significantly increasing the amount of trainable parameters. The world model stochastic state capacity can also be increased by using a larger number of groups and/or token dimensions. However, this results in a significantly larger number of parameters due to linear projections. In contrast, the spatial latent space benefits from weight sharing, which provides a useful position bias for the world model.

Temporal Masked Transformer Network EMERALD uses a Transformer State-Space Model (TSSM) (Chen et al., 2021) to learn long-range memory dependencies and predict future observations more accurately. The Transformer network uses masked self-attention with relative positional encodings (Dai et al., 2019), which simplifies the use of the world model during imagination and evaluation. We also use truncated backpropagation through time (TBTT) (Pašukonis et al., 2023) to preserve information over time. This requires the sampling of training trajectories sequentially in order to access past memory, passing cached attention keys and values from one batch to the next. The Transformer network outputs hidden states $h_t \in \mathbb{R}^{T \times D}$, carrying temporal information.

Spatial MaskGIT Predictor The MaskGIT predictor network uses a Transformer architecture with spatial attention to model relationships between spatial tokens. After spatial upsampling by the latent decoder network, the temporal hidden states serve as conditioning inputs to accurately predict the next spatial tokens. To train the MaskGIT predictor, we uniformly sample decoding times $\tau \in [0, 1]$ and use a cosine schedule to mask $N = \lfloor \gamma HWG \rfloor$ tokens from the latent space: $z_t^{mask} = z_t \odot m_t$ with mask $m \in \{0, 1\}^{H \times W \times G}$. The MaskGIT predictor learns to predict masked tokens by

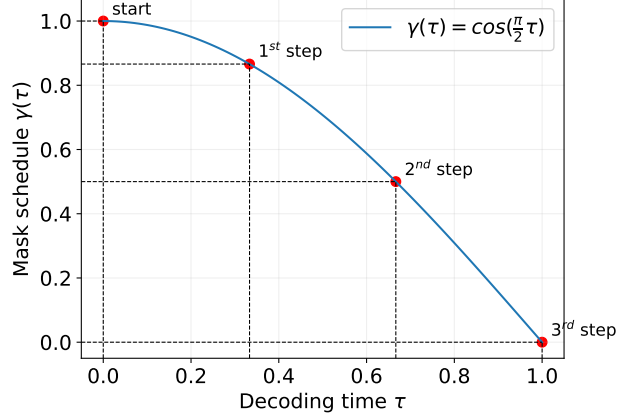


Figure 5: Cosine mask schedule. During training, we uniformly sample decoding times τ between 0 and 1. During imagination, the world model samples all masked tokens and refines $N = \lfloor \gamma HWG \rfloor$ tokens with lower probability. We illustrate the schedule used for $S = 3$ decoding steps.

minimizing the KL divergence with the unmasked latent state as follows:

$$L_{mask} = \text{KL} [sg(q_\phi(z_t | o_t)) \parallel p_\phi(\hat{z}_t | h_t, z_t^{mask})] \quad (2)$$

We use the stop gradient operator $sg(\cdot)$ to prevent the gradients of targets from being backpropagated.

In order to stabilize learning, the predictor also uses a dynamics loss with regularization (Hafner et al., 2023). A linear layer is optimized to predict the target latent states from upsampled hidden states. This allows to guide the predictions of the MaskGIT predictor in early training. The regularization terms stabilize learning by training the encoder representations to become more predictable. Both loss terms are scaled with loss weights $\beta_{dyn} = 0.5$ and $\beta_{reg} = 0.1$, respectively:

$$L_{dyn} = \beta_{dyn} \text{KL} [sg(q_\phi(z_t | o_t)) \parallel p_\phi(\hat{z}_t | h_t)] + \beta_{reg} \text{KL} [q_\phi(z_t | o_t) \parallel sg(p_\phi(\hat{z}_t | h_t))] \quad (3)$$

Decoder Network The decoder network receives both spatial latent states z_t and temporal hidden states h_t as inputs. This helps the encoder to learn more compressed representations by conditioning on past context. The two representations are projected and concatenated along the channel dimension for decoding. The reconstruction loss L_{rec} learns hidden representations for the world model by reconstructing input visual observations o_t as follows:

$$L_{rec} = \|\hat{o}_t - o_t\|^2 \quad (4)$$

Reward and Continuation Predictors L_{rew} and L_{con} train the world model to predict environment rewards and

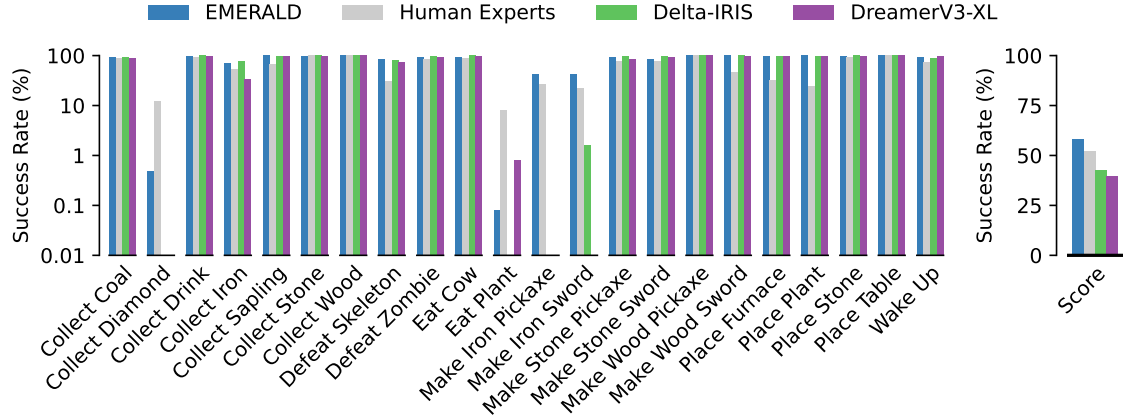


Figure 6: Achievements success rates over 256 evaluation episodes after training 10M environment steps. EMERALD succeeds to solve all achievements at least once. Our method also achieves new state-of-the-art performance, becoming the first method to surpass human experts performance in terms of achievements score.

episode continuation flags, which are used to compute the returns of imagined trajectories during the imagination phase. We adopt the symlog cross-entropy loss from DreamerV3 (Hafner et al., 2023), which scales and transforms rewards into twohot encoded targets to ensure robust learning across games with different reward magnitudes:

$$L_{rew} = \text{SymlogCrossEnt}(\hat{r}_t, r_t) \quad (5a)$$

$$L_{con} = \text{BinaryCrossEnt}(\hat{c}_t, c_t) \quad (5b)$$

Complete Training Objective Given an input batch containing B sequences of T image observations $o_{1:T}$, actions $a_{1:T}$, rewards $r_{1:T}$, and episode continuation flags $c_{1:T}$, the world model parameters (ϕ) are optimized to minimize the following loss function:

$$L(\phi) = \frac{1}{T} \sum_{t=1}^T \left[L_{mask} + L_{dyn} + L_{rew} + L_{con} + L_{rec} \right] \quad (6)$$

3.2. World Model Imagination Process

The agent critic and actor networks are trained with imaginary trajectories generated from the world model. Learning takes place entirely in latent space, which allows the agent to process large batch sizes and increase generalization. We flatten the model states of the sampled sequences along the batch and time dimensions to generate $B^{img} = B \times T$ sample trajectories using the world model. The self-attention keys and values features computed during the world model training phase are cached to be reused during the agent behavior learning phase and preserve past context. As shown in Figure 3b, the world model imagines $H = 15$ steps into the future using the Transformer network and the dynamics network head, selecting actions by sampling from the actor network categorical distribution. We detail the behavior learning process in more detail in the appendix A.6.

4. Experiments

In this section, we describe our experiments on the Crafter benchmark. We show the results obtained by EMERALD in Table 2. We also perform an ablation study on the world model architecture in section 4.3. Finally, we analyze the impact of the number of decoding steps on world model predictions in section 4.4. Additional comparison on the Atari 100k benchmark with other model-based methods can be found in the appendix A.7.

4.1. Crafter Benchmark

The Crafter benchmark was proposed in Hafner (2022) to evaluate a wide range of general abilities within a single environment. Crafter is inspired by the video game Minecraft. It features visual inputs, a discrete action space of 17 different actions and non-deterministic environment dynamics. The goal of the agent is to achieve as many achievements as possible among a list of 22 achievements¹. The benchmark evaluates the capacity of the agent to use long-term memory and accurate visual perception to collect resources and craft items while surviving in a hostile environment. The agents receive a single reward of +1 for each unlocked achievement. It also perceives a reward of -0.1 for every health point lost and a reward of +0.1 for every health point that is regenerated. The benchmark compares the achievements score, which is computed as the geometric mean of success rates for all 22 achievements. This metric prioritizes general agents that unlock a wide range of achievements over those that unlock a small number of achievements very frequently. The mean episode return can also be used to

¹ $Score (\%) = \exp\left(\frac{1}{N} \sum_{i=1}^N \ln(1 + s_i)\right) - 1$, where $s_i \in [0; 100]$ are the $N = 22$ achievement success rates.

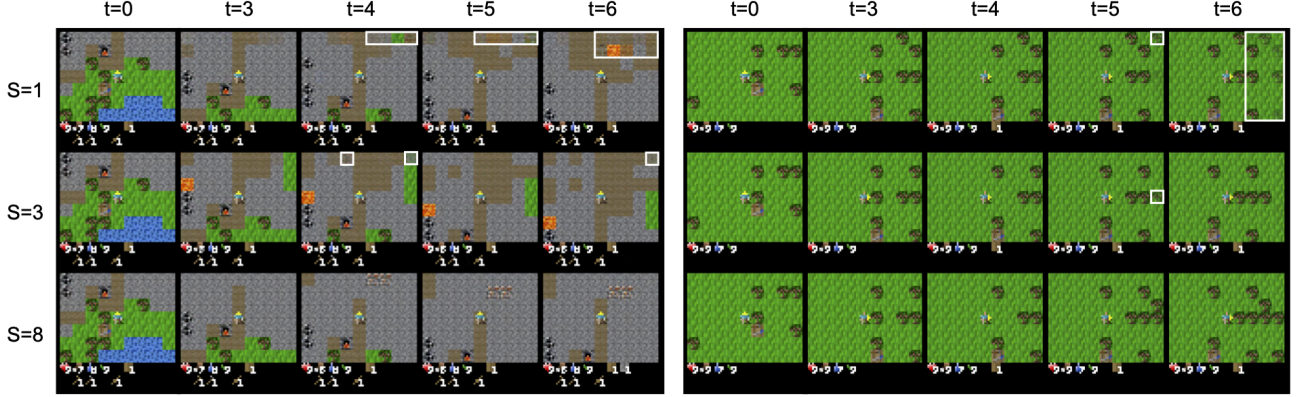


Figure 7: Impact of the number of decoding steps on world model prediction accuracy and efficiency. The randomness of the Crafter environment requires the world model to make refinements on the predicted tokens to avoid the sampling of tokens with contradictory representations. White rectangle boundaries show hallucinations due to incoherent predictions made during imagination. We use $S = 3$ decoding steps during imagination to achieve good prediction accuracy and efficiency.

directly compare the metric optimized during training.

Table 2: Crafter benchmark comparison (10M env frames). We show achievement scores and environment mean returns aggregated over 5 different seeds. Following [Micheli et al. \(2024\)](#), we also compute FPS as the total number of environment frames collected divided by the training duration.

Method	Score (%)	Return	#Params	FPS
Human Experts	50.5	14.3 ± 2.3	-	-
DreamerV3 (M)	34.9	14.0 ± 0.4	37M	38
DreamerV3 (XL)	39.6	15.4 ± 0.1	200M	23
Δ -IRIS	42.5	16.1 ± 0.1	25M	12
EMERALD (Ours)	58.1	16.8 ± 0.6	30M	27

4.2. Results

Table 2 compares the performance of EMERALD with Δ -IRIS and DreamerV3 on the Crafter benchmark after training 10M environment steps. We show achievements scores, mean episode returns and total number of parameters. Analogously to [Micheli et al. \(2024\)](#), we also compare the number of collected Frames Per Second (FPS) using a single RTX 3090 GPU for training. EMERALD achieves a score of 58.1%, being the first algorithm to exceed human experts performance on the benchmark. EMERALD’s enhanced perception enables the agent to detect objects and enemies more effectively, leading to increased survival time and improved performance. Our method also benefits from reduced training time compared to Δ -IRIS and DreamerV3 XL. The MaskGIT prior reduces decoding time during imagination while preserving the coherence of predicted tokens. Figure 6 compares the success rates of individual achievements. We find that EMERALD successfully solves all achievements

at least once when evaluating on 256 episodes. The agent progressively learns to master all levels of the technology tree, leading to the collection of diamonds.

4.3. Ablation Study

We study the impact of using spatial latent states and a Transformer-based world model on performance and training efficiency. Table 3 shows the performance obtained by each ablation, applying one modification at a time. We first experiment replacing the DreamerV3 vector latent space by a spatial latent space with MaskGIT predictions. We find that the use of a spatial latent state significantly helps to reduce reconstruction error and increase performance. This improves world model accuracy by encoding important environment details for the agent in the latent space. We then compare the use of a Transformer-based world model with masked self-attention with the recurrent-based world model of DreamerV3. We find that attention helps to further improve performance by conditioning representations on a longer context. The capacity of self-attention to model temporal relationships without recurrence makes the Transformer architecture highly effective at capturing historical context. The use of a Transformer-based architecture also improves training efficiency by not requiring recurrent processing of hidden states during the world model forward.

4.4. Choice of the number of decoding steps

While parallel predictions allow the world model to significantly reduce decoding time, this can also generate unclear predictions with unmatching sets of tokens. The randomness of the Crafter environment requires the world model to make refinements on the predicted tokens to avoid the sampling of tokens with contradictory representations. To

Table 3: Ablation study on world model architecture and latent space size (10M environment frames). We compare model performance, training efficiency and reconstruction quality. The performance metrics are aggregated over 5 seeds.

World Model Architecture	Latent Space Size	MaskGIT	Score (%)	Return	#Params	FPS	Pixel L_2 loss
DreamerV3 (M) RSSM	32	No	34.9	14.0 ± 0.4	37M	38	0.000522
DreamerV3 (S) RSSM	$4 \times 4 \times 32$	Yes	40.4	15.8 ± 0.1	28M	20	0.000231
EMERALD TSSM	32	No	31.8	13.1 ± 0.5	30M	44	0.000890
	$4 \times 4 \times 32$	Yes	58.1	16.8 ± 0.6	30M	27	0.000241

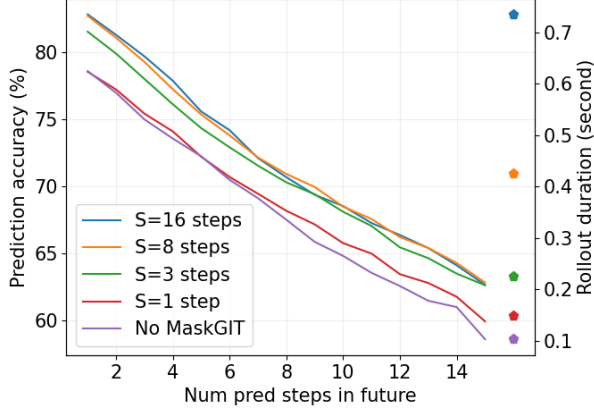


Figure 8: World model prediction accuracy. We show the token prediction accuracy for world model rollout aggregated over 5 seeds for several numbers of decoding steps.

avoid incoherent predictions, we follow MaskGIT by using multiple decoding steps during the imagination phase. Figure 7 shows the impact of the number of decoding steps on prediction quality. We find that using a single decoding step, without revising the prediction, can generate blurry predictions. These unmatching representations in latent space cause the world model to make incoherent predictions for successive time steps. Using a small number of decoding steps helps to revise the prediction and limit this effect while maintaining good prediction efficiency. Therefore, we set $S = 3$ decoding steps in our experiments.

Figure 8 shows the average accuracy of predictions for different numbers of decoding steps at imaginations time (No MaskGIT designates predictions made by the linear head learned by the dynamics loss L_{dyn}). The accuracy is averaged of the 5 EMERALD seeds and computed by comparing the target future states with predicted states during rollout, conditioned on the correct sequence of future actions. We find that using less than 3 decoding steps during imagination results in a drop of accuracy. We also compare the rollout time in seconds required to imagine 15 time steps in the future. Using a larger number of decoding steps can lead to a small increase in accuracy but also results in longer rollout

duration, which impacts training efficiency. We performed a corresponding ablation to study the impact of the number of imagination decoding steps on final performance over 5 seeds. Table 4 shows the impact on final performance when using different numbers of decoding steps for imagination. We find that the decrease of prediction accuracy has a noticeable impact on final performance. The decrease of average accuracy in world model predictions leads to the generation of less accurate trajectories for the actor and critic networks. Our experiments using 3 and 8 decoding steps achieves higher returns and achievement scores compared to using a single decoding step or a simple linear head for prediction.

Table 4: Impact of the number of world model decoding steps S on final performance and training efficiency.

#Decoding Steps	Score (%)	Return	FPS
No MaskGIT	51.6	16.1 ± 0.7	33
$S = 1$ step	53.8	16.1 ± 0.5	33
$S = 3$ steps	58.1	16.8 ± 0.6	27
$S = 8$ steps	55.1	16.5 ± 0.6	23

5. Conclusion

We propose EMERALD, a Transformer model-based reinforcement learning algorithm using a spatial latent state with MaskGIT predictions to generate accurate trajectories in latent space and improve the agent performance. EMERALD achieves new state-of-the-art performance on the Crafter benchmark with a budget of 10M environment steps, becoming the first method to exceed human experts performance. We study the impact of latent space size and find that the use of a spatial latent state helps the world model to perceive environment details that are crucial to the agent. Additionally, we demonstrate that a Transformer-based architecture outperforms a recurrent-based approach by leveraging attention to model long-range dependencies more effectively. Based on these findings, we hope this work will inspire researchers to further explore the impact of masked latent world models in more complex environments, such as Minecraft.

Acknowledgments

This work was partly supported by The Alexander von Humboldt Foundation (AvH).

Impact Statement

The development of autonomous agents for real-world applications introduces various safety and environmental concerns. In real-world scenarios, an agent might cause harm to individuals and damage to its surroundings during both training and deployment. Although using world models during training can mitigate these risks by allowing policies to be learned through simulation, some risks may still persist. This statement aims to inform users of these potential risks and emphasize the importance of AI safety in the application of autonomous agents to real-world scenarios.

References

Alonso, E., Jolley, A., Micheli, V., Kanervisto, A., Storkey, A. J., Pearce, T., and Fleuret, F. Diffusion for world modeling: Visual details matter in atari. *Advances in Neural Information Processing Systems*, 37:58757–58791, 2024.

Ba, J. L., Kiros, J. R., and Hinton, G. E. Layer normalization. *arXiv preprint arXiv:1607.06450*, 2016.

Bellemare, M. G., Naddaf, Y., Veness, J., and Bowling, M. The arcade learning environment: An evaluation platform for general agents. *Journal of artificial intelligence research*, 47:253–279, 2013.

Bengio, Y., Léonard, N., and Courville, A. Estimating or propagating gradients through stochastic neurons for conditional computation. *arXiv preprint arXiv:1308.3432*, 2013.

Chang, H., Zhang, H., Jiang, L., Liu, C., and Freeman, W. T. Maskgit: Masked generative image transformer. In *Proceedings of the IEEE/CVF Conference on Computer Vision and Pattern Recognition*, pp. 11315–11325, 2022.

Chen, C., Yoon, J., Wu, Y.-F., and Ahn, S. Transdreamer: Reinforcement learning with transformer world models. In *Deep RL Workshop NeurIPS 2021*, 2021.

Cho, K., van Merriënboer, B., Gulcehre, C., Bougares, F., Schwenk, H., and Bengio, Y. Learning phrase representations using rnn encoder-decoder for statistical machine translation. In *Conference on Empirical Methods in Natural Language Processing (EMNLP 2014)*, 2014.

Dai, Z., Yang, Z., Yang, Y., Carbonell, J. G., Le, Q., and Salakhutdinov, R. Transformer-xl: Attentive language models beyond a fixed-length context. In *Proceedings of the 57th Annual Meeting of the Association for Computational Linguistics*, pp. 2978–2988, 2019.

Esser, P., Rombach, R., and Ommer, B. Taming transformers for high-resolution image synthesis. In *Proceedings of the IEEE/CVF Conference on Computer Vision and Pattern Recognition*, pp. 12873–12883, 2021.

Guss, W. H., Codel, C., Hofmann, K., Houghton, B., Kuno, N., Milani, S., Mohanty, S., Liebana, D. P., Salakhutdinov, R., Topin, N., et al. The minerl 2019 competition on sample efficient reinforcement learning using human priors. *arXiv preprint arXiv:1904.10079*, 2019.

Ha, D. and Schmidhuber, J. Recurrent world models facilitate policy evolution. *Advances in Neural Information Processing Systems*, 31, 2018.

Hafner, D. Benchmarking the spectrum of agent capabilities. In *International Conference on Learning Representations*, 2022.

Hafner, D., Lillicrap, T., Fischer, I., Villegas, R., Ha, D., Lee, H., and Davidson, J. Learning latent dynamics for planning from pixels. In *International Conference on Machine Learning*, pp. 2555–2565. PMLR, 2019.

Hafner, D., Lillicrap, T., Ba, J., and Norouzi, M. Dream to control: Learning behaviors by latent imagination. In *International Conference on Learning Representations*, 2020.

Hafner, D., Lillicrap, T., Norouzi, M., and Ba, J. Mastering atari with discrete world models. In *International Conference on Learning Representations*, 2021.

Hafner, D., Pasukonis, J., Ba, J., and Lillicrap, T. Mastering diverse domains through world models. *arXiv preprint arXiv:2301.04104*, 2023.

Kaiser, L., Babaeizadeh, M., Milos, P., Osinski, B., Campbell, R. H., Czechowski, K., Erhan, D., Finn, C., Koza-kowski, P., Levine, S., et al. Model-based reinforcement learning for atari. In *International Conference on Learning Representations*, 2020.

Karras, T., Aittala, M., Aila, T., and Laine, S. Elucidating the design space of diffusion-based generative models. *Advances in Neural Information Processing Systems*, 35: 26565–26577, 2022.

Kingma, D. P. and Welling, M. Auto-encoding variational bayes. In *International Conference on Learning Representations*, 2014.

LeCun, Y., Bengio, Y., and Hinton, G. Deep learning. *nature*, 521(7553):436–444, 2015.

Lee, D., Kim, C., Kim, S., Cho, M., and HAN, W. S. Draft-and-revise: Effective image generation with contextual rq-transformer. *Advances in Neural Information Processing Systems*, 35:30127–30138, 2022.

Meo, C., Lica, M., Ikram, Z., Nakano, A., Shah, V., Didolkar, A. R., Liu, D., Goyal, A., and Dauwels, J. Masked generative priors improve world models sequence modelling capabilities. *arXiv preprint arXiv:2410.07836*, 2024.

Micheli, V., Alonso, E., and Fleuret, F. Transformers are sample-efficient world models. In *International Conference on Learning Representations*, 2023.

Micheli, V., Alonso, E., and Fleuret, F. Efficient world models with context-aware tokenization. In *International Conference on Machine Learning*, pp. 35623–35638. PMLR, 2024.

Pašukonis, J., Lillicrap, T. P., and Hafner, D. Evaluating long-term memory in 3d mazes. In *International Conference on Learning Representations*, 2023.

Ramesh, A., Pavlov, M., Goh, G., Gray, S., Voss, C., Radford, A., Chen, M., and Sutskever, I. Zero-shot text-to-image generation. In *International Conference on Machine Learning*, pp. 8821–8831. PMLR, 2021.

Robine, J., Höftmann, M., Uelwer, T., and Harmeling, S. Transformer-based world models are happy with 100k interactions. In *International Conference on Learning Representations*, 2023.

Schrittwieser, J., Antonoglou, I., Hubert, T., Simonyan, K., Sifre, L., Schmitt, S., Guez, A., Lockhart, E., Hassabis, D., Graepel, T., et al. Mastering atari, go, chess and shogi by planning with a learned model. *Nature*, 588(7839): 604–609, 2020.

Schulman, J., Wolski, F., Dhariwal, P., Radford, A., and Klimov, O. Proximal policy optimization algorithms. *arXiv preprint arXiv:1707.06347*, 2017.

Schwarzer, M., Ceron, J. S. O., Courville, A., Bellemare, M. G., Agarwal, R., and Castro, P. S. Bigger, better, faster: Human-level atari with human-level efficiency. In *International Conference on Machine Learning*, pp. 30365–30380. PMLR, 2023.

Sohl-Dickstein, J., Weiss, E., Maheswaranathan, N., and Ganguli, S. Deep unsupervised learning using nonequilibrium thermodynamics. In *International Conference on Machine Learning*, pp. 2256–2265. PMLR, 2015.

Sutton, R. S. Dyna, an integrated architecture for learning, planning, and reacting. *ACM Sigart Bulletin*, 2(4):160–163, 1991.

Tassa, Y., Doron, Y., Muldal, A., Erez, T., Li, Y., Casas, D. d. L., Budden, D., Abdolmaleki, A., Merel, J., Lefrancq, A., et al. Deepmind control suite. *arXiv preprint arXiv:1801.00690*, 2018.

Van Den Oord, A., Vinyals, O., et al. Neural discrete representation learning. *Advances in Neural Information Processing Systems*, 30, 2017.

Wang, S., Liu, S., Ye, W., You, J., and Gao, Y. Efficientzero v2: Mastering discrete and continuous control with limited data. In *International Conference on Machine Learning*, pp. 51041–51062. PMLR, 2024.

Williams, R. J. Simple statistical gradient-following algorithms for connectionist reinforcement learning. *Machine learning*, 8:229–256, 1992.

Yan, W., Hafner, D., James, S., and Abbeel, P. Temporally consistent transformers for video generation. In *International Conference on Machine Learning*, pp. 39062–39098. PMLR, 2023.

Zhang, W., Wang, G., Sun, J., Yuan, Y., and Huang, G. Storm: Efficient stochastic transformer based world models for reinforcement learning. *Advances in Neural Information Processing Systems*, 36, 2024.

A. Appendix

A.1. Latent Space Comparison

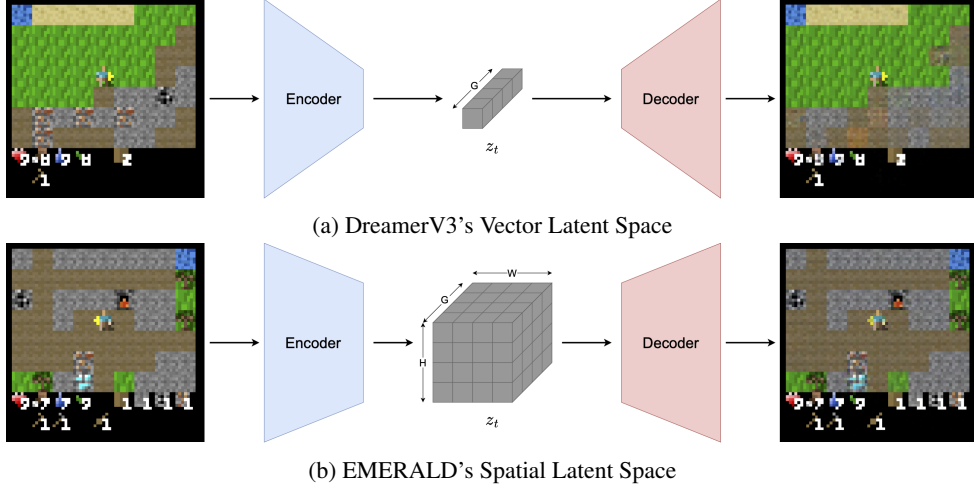


Figure 9: Comparison between the standard DreamerV3 vector latent space and EMERALD spatial latent space. We illustrate the size of each grouped latent space in tokens, where each token is of dimension D/G . The compressed nature of the DreamerV3 vector latent space $z_t \in \mathbb{R}^{G \times (D/G)}$ can result in the loss of crucial information, negatively impacting the agent’s performance. In contrast, the use of a spatial latent state $z_t \in \mathbb{R}^{H \times W \times G \times (D/G)}$ improves world model accuracy and provides further information to the agent.

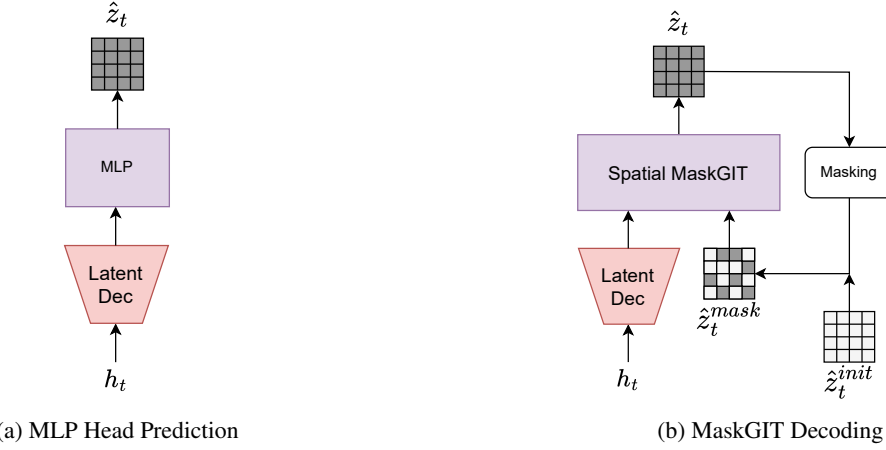


Figure 10: Comparison between standard MLP head and MaskGIT for decoding. The MLP head is very efficient and samples predictions without refinements, which can lead to ambiguous predictions with tokens having unmatching representations. MaskGIT limits this effect by progressively sampling and refining the prediction to avoid incoherent representations.

A.2. Success Rates Comparison

Table 5: Success rates of each method on the Crafter benchmark (10M environment steps).

Achievement	Human Experts	DreamerV3 (M)	DreamerV3 (XL)	Δ-IRIS	EMERALD
Collect Coal	86.0%	77.3%	86.8%	90.6%	91.6%
Collect Diamond	12.0%	0.0%	0.0%	0.0%	0.5%
Collect Drink	92.0%	93.0%	96.2%	98.4%	95.8%
Collect Iron	53.0%	12.1%	32.6%	76.6%	71.2%
Collect Sapling	67.0%	86.3%	97.0%	96.9%	99.9%
Collect Stone	100.0%	95.4%	98.2%	98.4%	97.9%
Collect Wood	100.0%	99.9%	99.9%	100.0%	99.8%
Defeat Skeleton	31.0%	50.5%	74.3%	81.3%	82.3%
Defeat Zombie	84.0%	87.6%	92.4%	96.9%	92.3%
Eat Cow	89.0%	84.1%	94.9%	98.4%	90.5%
Eat Plant	8.0%	0.4%	0.8%	0.0%	0.1%
Make Iron Pickaxe	26.0%	0.0%	0.0%	0.0%	41.5%
Make Iron Sword	22.0%	0.0%	0.0%	1.6%	41.6%
Make Stone Pickaxe	78.0%	72.0%	84.2%	95.3%	93.7%
Make Stone Sword	78.0%	80.3%	91.0%	95.3%	83.5%
Make Wood Pickaxe	100.0%	96.5%	98.6%	98.4%	99.2%
Make Wood Sword	45.0%	90.0%	96.9%	98.4%	98.8%
Place Furnace	32.0%	90.0%	96.0%	95.3%	96.2%
Place Plant	24.0%	86.3%	97.0%	96.9%	99.9%
Place Stone	90.0%	94.8%	98.2%	98.4%	97.4%
Place Table	100.0%	99.3%	99.9%	98.4%	99.4%
Wake Up	73.0%	92.2%	98.0%	89.1%	92.2%
Score	50.5%	34.9%	39.6%	42.5%	58.1%

A.3. Crafter Achievement Curves

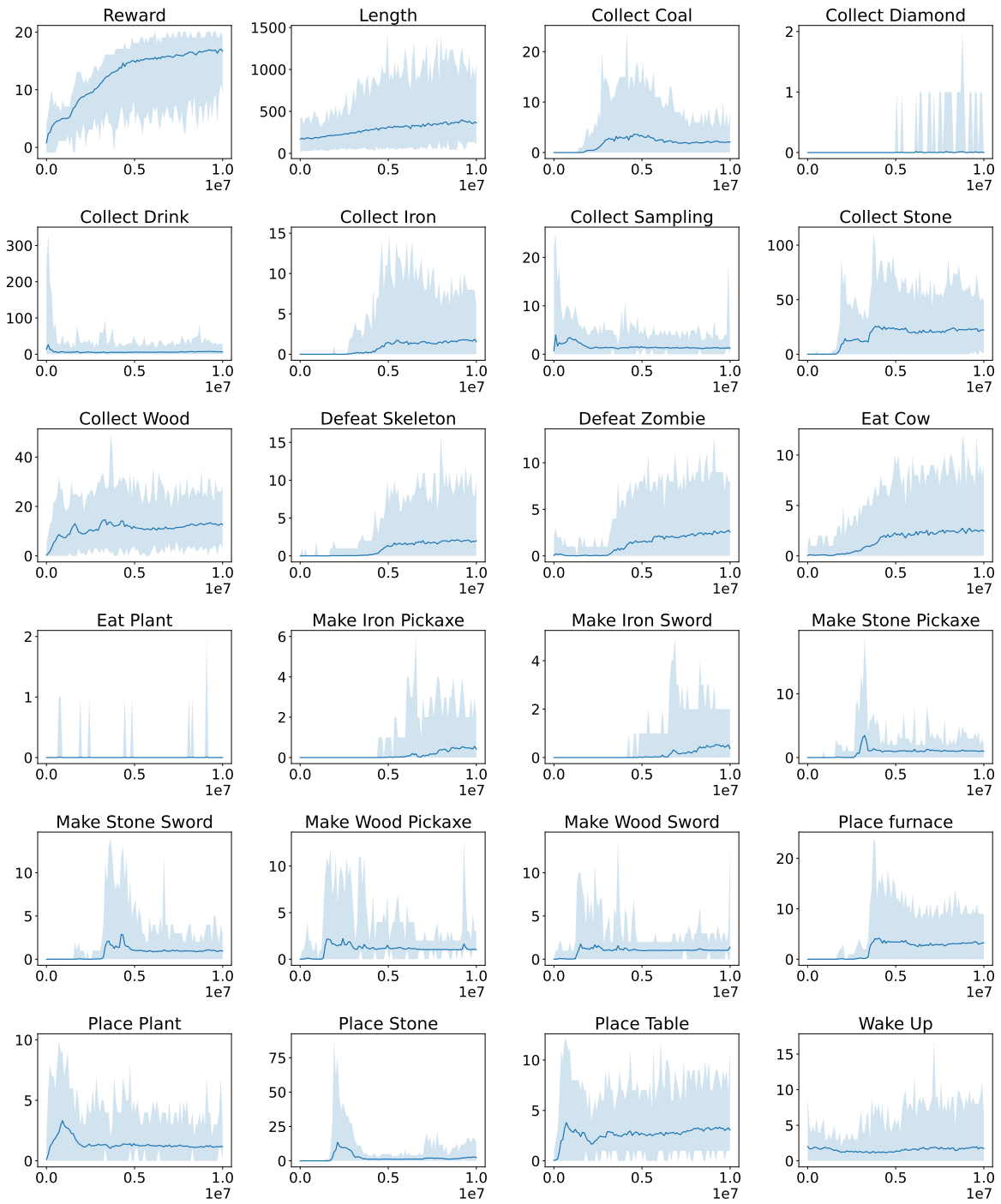


Figure 11: Achievement counts of EMERALD with shaded min and max.

A.4. Model Architecture

Table 6: Architecture of the encoder and decoder networks. The size of submodules is omitted and can be derived from output shapes. We use layer normalization (LN) and a SiLU activation layer inside residual blocks.

Encoder submodules	Output shape
Input image (o_t)	$64 \times 64 \times 3$
Conv strided	$32 \times 32 \times 32$
Residual block	$32 \times 32 \times 32$
Conv strided	$16 \times 16 \times 64$
Residual block	$16 \times 16 \times 64$
Conv strided	$8 \times 8 \times 128$
Residual block	$8 \times 8 \times 128$
Conv strided	$4 \times 4 \times 256$
Residual block	$4 \times 4 \times 256$
Conv	$4 \times 4 \times 1024$
Reshape + Softmax	$4 \times 4 \times 32 \times 32$
Sample + One Hot (outputs z_t)	$4 \times 4 \times 32 \times 32$

Decoder submodules	Output shape
Input latent state (z_t)	$4 \times 4 \times 32 \times 32$
Reshape (label as x_z)	$4 \times 4 \times 1024$
Input hidden state (h_t)	512
Linear + Reshape	$4 \times 4 \times 128$
Conv (label as x_h)	$4 \times 4 \times 256$
Concat x_z and x_h	$4 \times 4 \times 1280$
Conv	$4 \times 4 \times 256$
Residual block	$4 \times 4 \times 256$
Conv transposed	$8 \times 8 \times 128$
Residual block	$8 \times 8 \times 128$
Conv transposed	$16 \times 16 \times 64$
Residual block	$16 \times 16 \times 64$
Conv transposed	$32 \times 32 \times 32$
Residual block	$32 \times 32 \times 32$
Conv transposed (outputs \hat{o}_t)	$64 \times 64 \times 3$

Table 7: Transformer network. The latent states $z_{0:T-1}$ and one-hot encoded actions $a_{0:T-1} \in \mathbb{R}^{T \times A}$ are combined using an action mixer network (Zhang et al., 2024). The features are processed by the Transformer network to compute temporal hidden states $h_{1:T}$.

Submodule	Module alias	Output shape
Inputs latent states ($z_{0:T-1}$)	Latent Encoder	$T \times 4 \times 4 \times 32 \times 32$
Reshape + Conv		$T \times 4 \times 4 \times 128$
Flatten + Linear		$T \times 512$
Concat actions ($a_{0:T-1}$)	Action Mixer	$T \times (512 + A)$
Linear + LN + SiLU		$T \times 512$
Linear + LN		$T \times 512$
Transformer block $\times K$	Transformer Network	$T \times 512$
Outputs hidden states ($h_{1:T}$)		$T \times 512$

Table 8: MaskGIT predictor. The latent states z_t are masked and concatenated with spatial hidden states. The features are processed by the Transformer network to predict masked tokens \hat{z}_t .

Submodule	Module alias	Output shape
Inputs hidden states (h_t)	Latent Decoder	512
Linear + Reshape		$4 \times 4 \times 128$
Conv		$4 \times 4 \times 256$
Concat masked latent states (z_t)	Latent Embedding	$4 \times 4 \times 1536$
Flatten + Linear		16×256
Add pos embeddings		16×256
Transformer block $\times K_{mask}$	MaskGIT	16×256
Linear		16×1024
Reshape + Softmax		$4 \times 4 \times 32 \times 32$
Sample + One Hot (outputs \hat{z}_t)	Predictor	$4 \times 4 \times 32 \times 32$

Table 9: World model predictors and actor-critic networks architecture. Each network first projects spatial latent states z_t into feature vectors for concatenation with hidden states h_t . Each Linear layer is followed by a layer normalization and SiLU activation except for the last layer which outputs distribution logits.

Predictor submodules	Output shape	Network	Output dim	Output Distribution
Inputs latent states (z_t)	$4 \times 4 \times 32 \times 32$	Reward predictor	255	Symlog Discrete
Reshape + Conv	$4 \times 4 \times 128$	Continue predictor	1	Bernoulli
Flatten + Linear	512	Critic network	255	Symlog Discrete
Concat hidden states (h_t)	1024	Actor network	A	One hot Categorical
Linear + LN + SiLU	512			
Linear + LN + SiLU	512			
Linear prediction layer	Output dim			

A.5. Model Hyperparameters

Table 10: EMERALD hyper-parameters.

Hyperparameter	Value
General	
Image resolution	64×64
Batch size (B)	16
Sequence length (T)	64
Optimizer	Adam
Environment parallel instances	16
Collected frames per training Step	16
Replay buffer capacity	1M
World model	
Latent space size ($H \times W \times G$)	$4 \times 4 \times 32$
Number categories per group	32
Temporal Transformer blocks	4
Temporal Transformer width	512
Spatial MaskGIT blocks	2
Spatial MaskGIT width	256
Number of attention heads	8
Dropout probability	0.1
Attention context length	64
Learning rate	10^{-4}
Gradient clipping	1000
Actor-critic	
Imagination horizon (H)	15
Number of decoding steps (S)	3
Return discount	0.997
Return lambda	0.95
Critic EMA Decay	0.98
Return normalization Momentum	0.99
Actor entropy Scale	$3 \cdot 10^{-4}$
Learning rate	$3 \cdot 10^{-5}$
Gradient clipping	100

A.6. Actor Critic Learning

Analogously to world model predictor networks, the actor and critic networks are designed as simple MLPs with a projection layer for the spatial latent states. The two network have parameter vectors (θ) and (ψ) , respectively.

$$\begin{aligned} \text{Actor Network: } & a_t \sim \pi_\theta(a_t | s_t) \\ \text{Critic Network: } & v_t \sim V_\psi(v_t | s_t) \end{aligned} \quad (7)$$

Critic Learning Following DreamerV3, the critic network learns to minimize the symlog cross-entropy loss with discretized λ -returns obtained from imagined trajectories with rewards and episode continuation flags predicted by the world model:

$$R_t^\lambda = \hat{r}_{t+1} + \gamma \hat{c}_{t+1} \left((1 - \lambda) V_\psi(s_{t+1}) + \lambda R_{t+1}^\lambda \right) \quad R_{H+1}^\lambda = V_\psi(s_{H+1}) \quad (8)$$

The critic does not use a target network but relies on its own predictions for estimating rewards beyond the prediction horizon. This requires stabilizing the critic by adding a regularizing term toward the outputs of its own EMA network $V_{\psi'}$. Equation 9 defines the critic network loss:

$$L_{critic}(\psi) = \frac{1}{H} \sum_{t=1}^H \left[\underbrace{\text{SymlogCrossEnt}(v_t, R_t^\lambda)}_{\text{discrete returns regression}} + \underbrace{\text{SymlogCrossEnt}(v_t, V_{\psi'}(s_t))}_{\text{critic EMA regularizer}} \right] \quad (9)$$

Actor Learning The actor network learns to select actions that maximize the predicted returns using Reinforce (Williams, 1992) while maximizing the policy entropy to ensure sufficient exploration during both data collection and imagination. The actor network loss is defined as follows:

$$L_{actor}(\theta) = \frac{1}{H} \sum_{t=1}^H \left[\underbrace{-sg(A_t^\lambda) \log \pi_\theta(a_t | s_t)}_{\text{reinforce}} - \underbrace{\eta H(\pi_\theta(a_t | s_t))}_{\text{entropy regularizer}} \right] \quad (10)$$

Where $A_t^\lambda = (\hat{R}_t^\lambda - V_\psi(s_t)) / \max(1, S)$ defines advantages computed using normalized returns. The returns are scaled using exponentially moving average statistics of their 5th and 95th batch percentiles to ensure stable learning across all Atari games:

$$S = \text{EMA}(\text{Per}(R_t^\lambda, 95) - \text{Per}(R_t^\lambda, 5), \text{momentum} = 0.99) \quad (11)$$

A.7. Atari 100k Benchmark

The commonly used Atari 100k benchmark was proposed in Kaiser et al. (2020) to evaluate reinforcement learning agents on Atari games in low data regime. The benchmark includes 26 Atari games with a budget of 400k environment frames, amounting to 100k interactions between the agent and the environment using the default action repeat setting. This amount of environment steps corresponds to about two hours (1.85 hours) of real-time play, representing a similar amount of time that a human player would need to achieve reasonably good performance.

We evaluate our method on the benchmark to assess EMERALD’s performance on environments that do not necessarily require the use of spatial latents to achieve near perfect reconstruction. We also demonstrate improved training efficiency compared to Δ -IRIS and DIAMOND. Following preceding works, we use human-normalized metrics and compare the mean and median returns across all 26 games. The human-normalized scores are computed for each game using the scores achieved by a human player and the scores obtained by a random policy: $\text{normed score} = \frac{\text{agent score} - \text{random score}}{\text{human score} - \text{random score}}$.

The current state-of-the-art is held by EfficientZero V2 (Wang et al., 2024), which uses Monte-Carlo Tree Search to select the best action at every time step. Another recent notable work is BBF (Schwarzer et al., 2023), a model-free agent using learning techniques that are orthogonal to our work such as periodic network resets and hyper-parameters annealing to improve performance. In this work, to ensure fair comparison, we compare our method with model-based approaches that do not utilize look-ahead search techniques.

We compare EMERALD with Diamond (Alonso et al., 2024), Δ -IRIS (Micheli et al., 2024) and DreamerV3 (Hafner et al., 2023) as well as other model-based approaches like STORM (Zhang et al., 2024), IRIS (Micheli et al., 2023) and SimPLe (Kaiser et al., 2020). We find that EMERALD achieves comparable aggregated performance as Δ -IRIS and Diamond while offering higher training efficiency. When using a RTX 3090 GPU for training, EMERALD requires only 17 hours to reach 400k environment steps on the Breakout game while Δ -IRIS and DIAMOND need 27 hours and 75 hours, respectively.

Table 11: Agent scores and human-normalized metrics on the 26 games of the Atari 100k benchmark. We show average scores over 5 seeds. Bold numbers indicate best performing method for each game.

Game	Random	Human	SimPLe	TWM	IRIS	DreamerV3	STORM	Δ -IRIS	DIAMOND	EMERALD
Alien	228	7128	617	675	420	959	984	391	744	651
Amidar	6	1720	74	122	143	139	205	64	226	129
Assault	222	742	527	683	1524	706	801	1123	1526	798
Asterix	210	8503	1128	1116	854	932	1028	2492	3698	1045
Bank Heist	14	753	34	467	53	649	641	1148	20	927
Battle Zone	2360	37188	4031	5068	13074	12250	13540	11825	4702	15800
Boxing	0	12	8	78	70	78	80	70	87	71
Breakout	2	30	16	20	84	31	16	302	133	62
Chopper Command	811	7388	979	1697	1565	420	1888	1183	1370	990
Crazy Climber	10780	35829	62584	71820	59324	97190	66776	57854	99168	75380
Demon Attack	152	1971	208	350	2034	303	165	533	288	498
Freeway	0	30	17	24	31	0	34	31	33	31
Frostbite	65	4335	237	1476	259	909	1316	279	274	221
Gopher	258	2412	597	1675	2236	3730	8240	6445	5898	14702
Hero	1027	30826	2657	7254	7037	11161	11044	7049	5622	7655
James Bond	29	303	100	362	463	445	509	309	427	195
Kangaroo	52	3035	51	1240	838	4098	4208	2269	5382	8780
Krull	1598	2666	2205	6349	6616	7782	8413	5978	8610	7600
Kung Fu Master	258	22736	14862	24555	21760	21420	26182	21534	18714	22822
Ms Pacman	307	6952	1480	1588	999	1327	2673	1067	1958	1710
Pong	-21	15	13	19	15	18	11	20	20	20
Private Eye	25	69571	35	87	100	882	7781	103	114	100
Qbert	164	13455	1289	3331	746	3405	4522	1444	4499	1245
Road Runner	12	7845	5641	9107	9615	15565	17564	10414	20673	6620
Seaquest	68	42055	683	774	661	618	525	827	551	468
Up N Down	533	11693	3350	15982	3546	7600	7985	4072	3856	5227
# Superhuman	0	N/A	1	8	10	9	10	11	11	11
Normed Mean (%)	0	100	33	96	105	112	127	139	146	134
Normed Median (%)	0	100	13	51	29	49	58	53	37	51